

Performance evaluation of adsorptive removal of Ni(II) by treated waste granular-activated carbon and new granular-activated carbon

ZiJie Wang, Zheng Wang*, Kai Xu, Lei Chen, ZiZeng Lin, YaLi Liu

School of Civil Engineering, Nanjing Forestry University, Longpan Road 159#, Nanjing 210037, China, Tel. +86 25 85427691; emails: wangzheng@njfu.edu.cn (Z. Wang), wzj854333843@163.com (Z. Wang), horizonxk@163.com (K. Xu), clymcl@163.com (L. Chen), ccitlin@163.com (Z. Lin), liuyali0418@163.com (Y. Liu)

Received 19 October 2018; Accepted 17 April 2019

ABSTRACT

Granular-activated carbon is a commonly used adsorbent in water treatment. It can be reused by regeneration when saturated, but there are limits to the number of regenerations in actual engineering. This study created a simple and economical treatment method allowing for the reuse of waste granular-activated carbon (WGAC) that approaches the regeneration limit. The adsorption kinetics, equilibrium, and thermodynamics of Ni(II) onto the treated waste granular-activated carbon (TWGAC) and the new granular-activated carbon (NGAC) were studied. The N_2 adsorption/desorption isotherms, zeta potential, SEM, energy-dispersive spectrometry and FTIR spectra were used to characterize and compare the NGAC and TWGAC. Analysis revealed that the structure of WGAC was severely damaged, but the adsorption capacity and adsorption mechanism after treatment were similar to those of NGAC. Experimental data showed that the pseudo-second-order kinetic model and the Freundlich isothermal model had high correlation coefficients ($R^2 > 0.99$). The maximum adsorption capacity of TWGAC and NGAC was 138.9 and 123.5 $mg\ g^{-1}$. Thermodynamic parameters, including the negative values ΔG , positive values ΔH , and positive value ΔS , indicated that the current adsorption processes of TWGAC and NGAC were feasible, spontaneous and endothermic. After three cycles, TWGAC's removal rate for Ni(II) remained as high as 95.3%.

Keywords: Waste granular-activated carbon; Reuse; Ni(II) adsorption; Kinetics; Thermodynamics; Isotherms

1. Introduction

Ni(II) are heavy metal ions present in industrial wastewater, which have been attracting a worldwide attention due to their increasingly toxic effects on the environment and people [1]. The Ni(II) pollution mainly comes from the industrial applications such as mining, metallurgy, welding, battery manufacturing, electroless nickel plating, and electroplating. According to China's 'Electroplating Pollutant Emission Standard (GB 21900-2008)', the emission levels of nickel in China are strictly limited to 0.1 $mg\ L^{-1}$ [2]. Moreover, Ni(II) ions easily accumulate in live organisms.

Excess amount of Ni(II) ions can lead to lung embolism, neurological disorders, allergic dermatitis, as well as to an increased risk of developing lung, nose, larynx, and prostate cancers [3,4]. The World Health Organization (WHO) has set a maximum limit of 0.1 $mg\ L^{-1}$ of nickel in drinking water [5]. Therefore, it is essential to protect human and provide environmental safety and effectively remove Ni(II) ions from wastewater.

Several water treatment technologies, such as chemical precipitation, ion exchange, membrane separation, flocculation, and adsorption, have been used to eliminate Ni(II) ions from water [6–11]; however, none of them are perfect.

* Corresponding author.

For example, the resin cost of the ion exchange technology is high, and the regeneration solution needs additional treatment, which imposes certain limitations in practical engineering use [6]. Membrane separation technology has the potential for membrane fouling and requires frequent membrane cleaning to restore processing capacity. In addition, there are high costs associated with treatment of the concentrate [12]. Traditional flocculants have a poor heavy metal removal capacity and frequently require additional modification or compounding to enhance the removal process [13]. Although adsorption is a relatively traditional processing technique, compared with other technologies, it has the greatest development space and application prospects owing to its low cost, stability, and convenience.

Granular-activated carbon (GAC) is one of the most widely used adsorbent with a high surface area, variety of functional groups, good internal porosity, low cost, and efficient processing capability [14]. Importantly, the adsorption capacity of GAC is comparable with other adsorbents, and GAC loses its adsorption capacity when saturated. When spent, GAC is typically incinerated or used in the next adsorption cycle after regeneration [15]. However, the active surface and volume of the porous structure decrease with each GAC regeneration, resulting in its decreased adsorption capacity [16]. As a result, many research studies focus on optimizing activated carbon regeneration methods, including biological regeneration, microwave regeneration, oxidative regeneration or thermal regeneration [17–19]. However, regeneration is not unlimited, and GAC will eventually have to be discarded after repeated regeneration. Because the internal structure of the GAC after the regeneration limit is reached is severely damaged. The carbon content and porosity of the GAC are greatly reduced [20]. Water plants in China usually replace the old GAC with new granular-activated carbon (NGAC) 5 years after when GAC is first used. Biological activated carbon also needs to be regenerated after being used in drinking water treatment plants for 6 to 7 years [21]. The main reason is that the regeneration and transportation costs are relatively high, and the adsorption performance of GAC after regeneration is noticeably reduced. In contrast, the use of NGAC is more efficient and very easy. By developing a combination of ultrasonic cleaning and grinding, we can extend the lifespan of GAC that reaches the regeneration limit and is not otherwise suitable for typical regeneration. With this approach, the waste granular-activated carbon (WGAC) that was aimed for destruction can now be easily and effectively reused to remove environmental contamination due to heavy metal ions. At the same time, the ultrasonic cleaning and grinding process is simple and space efficient. It can be carried out inside the water plant, eliminating the need for expensive long-distance transportation. At present, we believe that there is no similar method that can reuse WGAC that is no longer suitable for regeneration.

The objectives of this study are as follows: (1) to evaluate the adsorption properties of Ni(II) on NGAC and the TWGAC, (2) to compare the surface properties of NGAC and TWGAC, (3) to fit experimental data through kinetic and thermodynamic models, and (4) to analyze the adsorption mechanism of Ni(II) on NGAC and TWGAC.

2. Materials and methods

2.1. Materials

The primary chemicals were all pure and of analytical grade, and the experimental water was deionized water. Nickel sulfate ($\text{NiSO}_4 \cdot 6\text{H}_2\text{O}$) was purchased from the Aladdin Shenghai Technology Co., Ltd. (Shanghai). Hydrochloric acid (HCl) and sodium hydroxide (NaOH) were purchased from the Nanjing Chemical Reagent Co., Ltd.

The NGAC and WGAC used in the experiment were coal-based GAC produced by Datong Yunguang Activated Carbon Co. Ltd. (Datong, Shanxi Province, China) WGAC was obtained from the Jitai Water Plant (Sihong County, Jiangsu Province, China) and has been in use for 5 years. The NGAC was ground into a powder and sieved through a sieve (200 mesh) to obtain a homogenous powder during the adsorption experiment.

2.2. Treatment of WGAC

The treatment method of WGAC was as follows: WGAC was washed with ultrasonic waves at 40 kHz for 10 min to remove suspended and washable contaminants (the volume of water is five times of WGAC). Then, the washed GAC was dried at 105°C to remove any volatile materials present within the pores of the grain. Afterwards, the dried GAC was placed in a crusher (Huangdai, 800Y, China) and ground for 2 min. Finally, it was sieved through a sieve (200 mesh) to obtain a homogenous powder. The used water was discharged as wastewater to the sewage treatment plant.

2.3. Characterization methods

The Brunauer–Emmett–Teller (BET) specific surface area, pore size distribution and pore volume were examined using a fully automatic specific surface area and pore size distribution meter (Micromeritics, ASAP2020 HD88, USA). The sample was measured for nitrogen adsorption/desorption isotherm at 77 K after degassing at 150°C for 24 h. The specific surface area was estimated using the BET equation in the range of p/p_0 is from 0.08 to 0.22. The specific surface area was estimated using the BET equation [22]. The pore size was estimated using the t -plots and the Barrett–Joyner–Halenda (BJH) equation [23]. The high-resolution images of the activated carbon were captured using an environmental scanning electron microscope (FEI, Quanta 200, USA). The accelerating voltage was 25 kV, and the images were taken at 600x and 2,400x magnification. No conductive layer of metal was added to the sample. Characterization of surface elements and chemical states of activated carbon were examined by X-ray energy-dispersive spectrometry (Oxford, INCA X-act, UK). The functional groups on the activated carbon were analyzed by Fourier transmission infrared spectroscopy (Thermo Scientific, Nicolet IS5, USA), by taking 32 scans from 400 to 4,000 cm^{-1} with a resolution of 2 cm^{-1} using the potassium bromide pellet technique. The weight proportion AC:KBr used for the preparation of the pellet for FTIR analysis is 1:150. The particle size and zeta potential of the activated carbon after grinding were analyzed by laser particle size analyzer (Malvern, ZS90, UK). The zeta potential determination procedure was as follows: 0.1 g of activated carbon

was placed in 100 mL of pure water and shaken. The pH was adjusted to 5, 5.5, 6, 6.5, 7, 7.5, 8, 8.5, 9 with HCl and NaOH. The prepared activated carbon suspension was allowed to stand for 5 min, and then the zeta potential was measured.

2.4. Adsorption experiments

The nickel sulfate was prepared as a stock solution in deionized water and 100 mL of the desired concentration of Ni(II) was mixed with NGAC and TWGAC. Afterwards, the pH was adjusted with 0.1 M NaOH and HCl solution and the mixture was left mixing at 150 rpm and specified time. Next, the mixture was filtered using a 0.45 μm filter and 20 mL of the supernatant was collected. The effect of adsorbent dose on the Ni(II) adsorption capacity of TWGAC and NGAC was studied at adsorption doses of 0.1, 0.2, 0.3, 0.4, and 0.5 g L^{-1} . In this experiment, the adsorbate concentration, temperature, contact time, and pH were controlled at 10 mg L^{-1} , 27°C, 75 min, and 8, respectively. The effect of pH on the Ni(II) adsorption capacity of TWGAC and NGAC was studied at a wide range of pH (5, 5.5, 6, 6.5, 7, 7.5, 8, 8.5, and 9). In this experiment, the initial adsorbate concentration, adsorbent dose, contact time, and temperature were controlled at 10 mg L^{-1} , 0.4 g L^{-1} , 75 min, and 27°C, respectively. The effect of contact time on the Ni(II) adsorption capacity of TWGAC and NGAC was studied at 15, 30, 45, 60, 75, and 90 min. In this experiment, the initial adsorbate concentration, adsorbent dose, temperature, and pH were controlled at 10 mg L^{-1} , 0.4 g L^{-1} , 27°C, and 8, respectively.

The residual Ni(II) concentration was determined by flame atomic absorption spectrophotometry using an atomic absorption spectrophotometer (Persee, TAS-990, China). The test solution was sprayed into an air-acetylene lean flame, resulting in the nickel compound disintegrating into a ground state atom at a high temperature. The atomic vapor produced selective absorption of the characteristic line 232 nm which was generated by the sharp line source (nickel hollow cathode lamp). At a lamp current of 12.5 mA, a spectral passband of 0.2 nm, an observed height of 8 mm, an acetylene flow rate of 2.2 L min^{-1} , and an air flux of 9.4 L min^{-1} , the absorbance was proportional to the concentration of nickel in the test solution. Adsorption experiments were performed in triplicate and reported as average data.

The adsorption capacity (Eq. (1)) and the percentage removal (Eq. (2)) of Ni(II) were determined as follows:

$$q = \frac{(C_0 - C_e)}{m} \times V \quad (1)$$

$$\% \text{Removal of Ni(II)} = \frac{C_0 - C_e}{C_0} \times 100 \quad (2)$$

where C_0 is the initial Ni(II) concentration (mg L^{-1}), C_e is the Ni(II) concentration at equilibrium (mg L^{-1}), V is the volume of solution (L), m is the mass of activated carbon (g), and q is the adsorption capacity (mg g^{-1}).

2.5. Adsorption kinetics

The study of adsorption kinetics aids in determining the mechanism of adsorption and reaction pathways.

For evaluating the adsorption kinetics of Ni(II) on NGAC and TWGAC, the pseudo-first-order (Eq. (3)), pseudo-second-order (Eq. (4)), and Elovich models (Eq. (5)) were applied to fit the experimental data. In addition, the accuracy of these models was evaluated by determining the nonlinear coefficient (R^2). The equations can be expressed as follows:

$$\ln(q_e - q_t) = \ln q_e - k_1 t \quad (3)$$

$$\frac{t}{q_t} = \frac{1}{k_2 q_e^2} + \frac{t}{q_e} \quad (4)$$

$$q_t = \frac{1}{\beta} \ln(\alpha\beta) + \frac{1}{\beta} \ln t \quad (5)$$

where q_e is the amount adsorbed at equilibrium (mg g^{-1}), q_t is the amount adsorbed at any time t (mg g^{-1}), t is the adsorption time (min), k_1 is the rate constant (min^{-1}), k_2 is the second-order rate constant ($\text{g mg}^{-1} \text{min}^{-1}$), α is the initial adsorption rate ($\text{mg g}^{-1} \text{min}^{-1}$), and β is the desorption constant (g mg^{-1}).

2.6. Adsorption isotherm

Adsorption isotherms play an important role in the assessment of the actual adsorption process. To determine the adsorption isotherm of Ni(II) on NGAC and TWGAC, Langmuir (Eq. (6)) and Freundlich models (Eq. (7)) were used to fit the experimental data. In addition, the accuracy of these models was evaluated by determining the nonlinear coefficient (R^2). The equations can be expressed as follows:

$$\frac{C_e}{q_e} = \frac{1}{q_m K_L} + \frac{C_e}{q_m} \quad (6)$$

$$\ln q_e = \ln K_F + \frac{1}{n} \ln C_e \quad (7)$$

where C_e is the equilibrium concentration (mg L^{-1}), q_e is the amount adsorbed at equilibrium (mg g^{-1}), q_m is the maximum concentration corresponding to monolayer (mg g^{-1}), K_L is the Langmuir adsorption constant (L mg^{-1}), K_F is the Freundlich constant ($\text{mg g}^{-1} (\text{L mg}^{-1})^{-1/n}$), and n is the heterogeneity factor denoting the adsorption intensity.

2.7. Adsorption thermodynamics

Adsorption thermodynamics can be used to describe the effects of temperature during adsorption. The thermodynamic parameters of adsorption process such as Gibbs free energy change (ΔG), enthalpy change (ΔH), and entropy change (ΔS) can be calculated as follows:

$$\Delta G = -RT \ln K \quad (8)$$

$$\Delta G = \Delta H - T\Delta S \quad (9)$$

where R is the ideal gas constant ($8.314 \text{ J mol}^{-1} \text{ K}^{-1}$), T is the absolute temperature (K), and K is the adsorption equilibrium constant obtained from the isotherms which

has a better fitting parameter. The ΔH and ΔS were obtained from the slope and intercept of the plot of ΔG vs. T . Adsorption experiments were carried out at 27°C, 37°C, and 47°C to evaluate temperature effects.

3. Results and discussion

3.1. Characteristics of TWGAC

Fig. 1 shows the nitrogen adsorption isotherms of NGAC and TWGAC at 77 K, which can be described as a type I isotherm. The line type of the type I isotherm has a micropore filling feature characterized by a rapid rise in the adsorption volume at low relative pressures, followed by a flat phase before finally reaching a limit. This indicates that the high specific surface area (893.37 and 924.69 m² g⁻¹) of TWGAC and NGAC is due to the higher number of micropores, which suggests that they are all microporous solids. According to the nitrogen adsorption isotherm, we calculated the specific surface area of the sample using the BET equation [24,25]. The sample micropore data were obtained by t-plot methods. The surface area, pore volume and average pore size of TWGAC and NGAC are shown in Table 1. TWGAC has a lower nitrogen adsorption compared with NGAC, which is consistent with the micropore volume in Table 1. Further, the specific surface area of TWGAC is much lower than that of NGAC, which may be due to the use of the water plant for 5 years. However, TWGAC still has great application potential.

The SEM images of NGAC and TWGAC at 600× and 2,400× magnification are shown in Fig. 2. The image of NGAC (Figs. 2a and b) indicates that it has a smooth surface and a dense structure. In addition, it also has multiple pores with uneven apertures, which are beneficial to the adsorption of heavy metal ions. In contrast, the damaged surface of TWGAC (Figs. 2c and d) was more complex. The surface became uneven and the structure of the activated carbon was very loose, which can be likely explained by damage during the 5 years of adsorption and soaking.

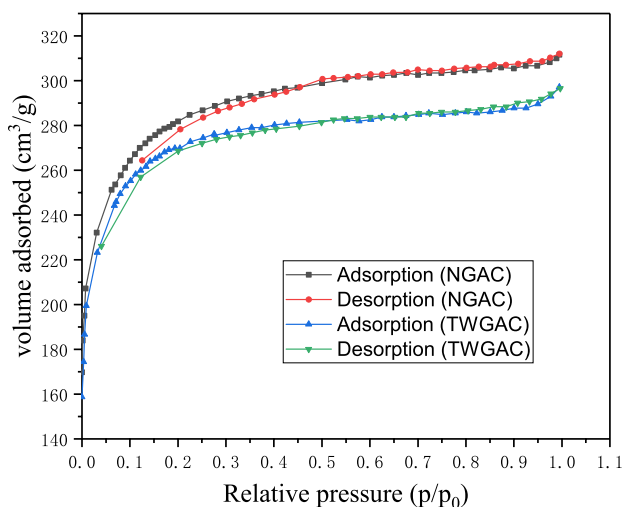


Fig. 1. Nitrogen adsorption–desorption isotherm of TWGAC and NGAC.

Table 1

Surface area, pore volume, average pore sizes, and average particle size of TWGAC and NGAC

Adsorbent	TWGAC	NGAC
BET surface area (m ² g ⁻¹)	893.37	924.69
Micropore surface area (m ² g ⁻¹)	588.49	666.69
Total pore volume (cm ³ g ⁻¹)	0.459	0.471
Micropore volume (cm ³ g ⁻¹)	0.365	0.388
Average pore size (nm)	2.053	2.034
Average particle size (nm)	462.8	635.4

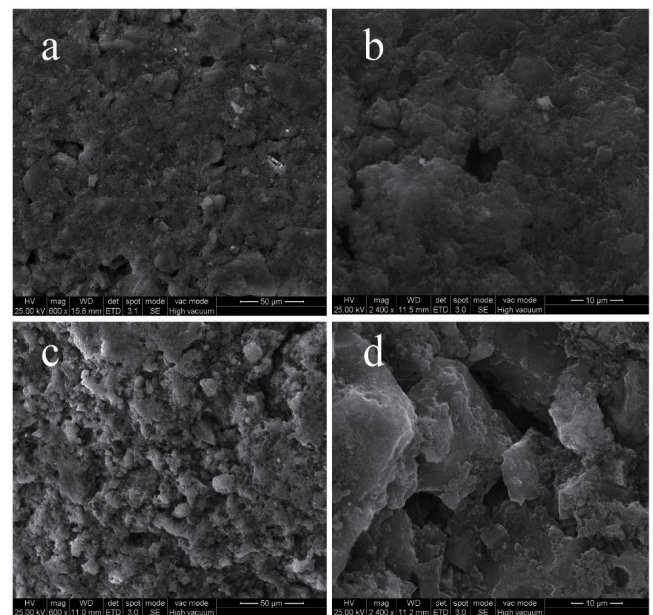


Fig. 2. SEM images of (a) NGAC at 600×; (b) NGAC at 2,400×; (c) TWGAC at 600×; (d) TWGAC at 2,400×.

In addition, the pores on the surface of the TWGAC become larger and some pores became pits. No suspended and washable contaminants were observed from the figure, which proved the effectiveness of ultrasonic cleaning to some extent. We observed that TWGAC still had some limited adsorption capacity left. However, owing to structural considerations and economic constraints, it was no longer suitable for regeneration through long-distance transportation. We concluded that the reuse of the powder after grinding can compensate for the defects in the structure and improve the treatment effect.

The composition change of NGAC and TWGAC was analyzed using the energy-dispersive spectrometry (EDS), as shown by images in Figs. 3a and b. The composition of TWGAC (Fig. 3b) was similar to that of the new-activated carbon (Fig. 3a) and was mainly composed of carbon and oxygen. The atomic % of the C elements in TWGAC and NGAC were 93.02% and 92.44%, respectively, and the atomic % of the O elements were 5.54% and 5.94%, respectively. The other elements had an atomic % less than 1. Not surprisingly, the composition of activated carbon did not change much during the 5 years of utilization. In addition, TWGAC did not

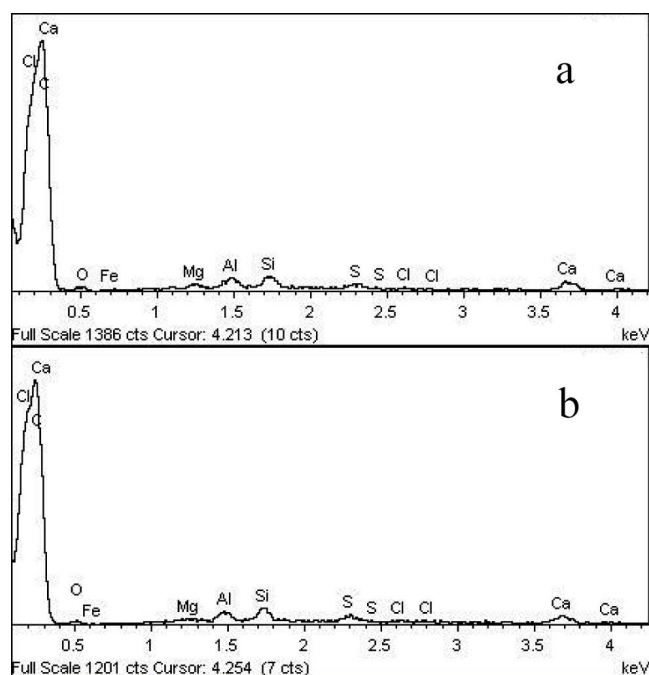


Fig. 3. EDS analysis of (a) NGAC and (b) TWGAC.

contain any toxic and hazardous substances after ultrasonic cleaning and could be used safely.

The FTIR spectra of NGAC and TWGAC are shown in Fig. 4a. The spectra indicate that NGAC and TWGAC have many similar absorption peaks. The absorption peak present at $3,400\text{ cm}^{-1}$ is $-\text{OH}$ associated with hydrogen bonding, where activated carbon adsorbed water [26,27]. Then, the absorption peaks present at $1,628$; $1,575$; and $1,385\text{ cm}^{-1}$ are associated with asymmetric vibrations of $\text{C}=\text{O}$ [28]. The absorption peaks at 980 and $1,100\text{ cm}^{-1}$ are weak, corresponding to phenolic hydroxyl groups [29]. However, the number of functional groups in TWGAC is lower compared with NGAC, indicating that the functional groups of TWGAC have likely changed during many years of use, and chemical bonds became broken. Overall, the TWGAC retained most of its functional groups and still possessed a good adsorption capacity.

The particle size distribution of NGAC and TWGAC is shown in Fig. 4b. It can be seen from the figure that the particle size distribution curves of NGAC and TWGAC basically conform to the normal distribution. The average particle size of NGAC is 635.4 nm , and most of the particle size ranges from 500 to $1,000\text{ nm}$. TWGAC has a smaller average particle size (462.8 nm) and particle size range (200 – 500 nm) compared with NGAC. This may be due to the loose structure of TWGAC after prolonged use and soaking, so it is easier to grind than NGAC.

The zeta potential of NGAC and TWGAC at different pH is shown in Fig. 4c. The graph shows that the zeta potential changes of NGAC and TWGAC have the same trend at different pH. The zeta potential of NGAC and TWGAC is negative at pH 5 – 9 , indicating that both surfaces are negatively charged at this time. As the pH increases, the absolute value of both zeta potentials increases. When the pH is

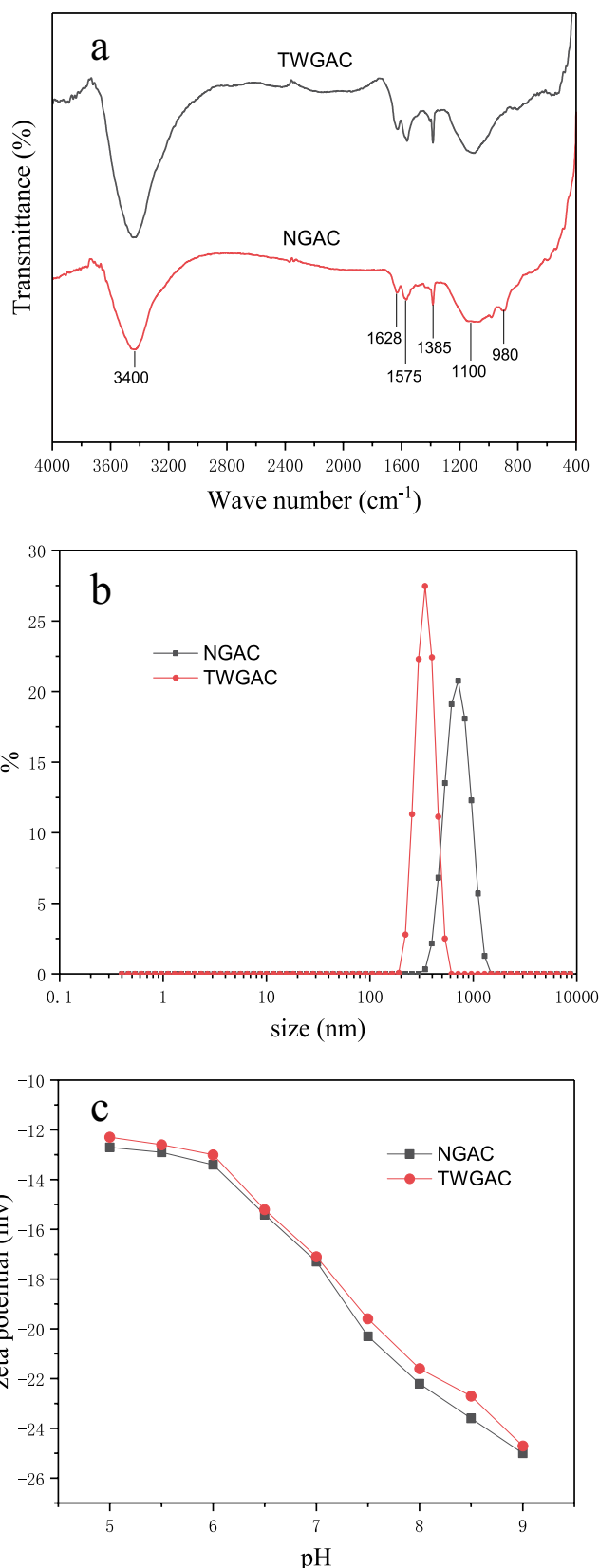


Fig. 4. (a) FT-IR spectra of TWGAC and NGAC; (b) particle size distribution of TWGAC and NGAC; (c) zeta potential of TWGAC and NGAC.

increased from 5 to 9, both zeta potentials are doubled, so the change in pH has a significant effect on the zeta potential.

3.2. Effect of adsorbent dose on TWGAC and NGAC

One of the key parameters determining the properties of adsorption is adsorbent dose. The relationship between the removal rate of Ni(II) and adsorbent dose is shown in Fig. 5a. The effect of adsorbent dose on TWGAC and NGAC was the same throughout the entire process. As the amount of TWGAC and NGAC increased from 0.1 to 0.4 g L⁻¹, the removal rate of Ni(II) gradually increased from 98.2% to 99.47%. This occurred because the effective adsorption sites increased with the increased amount of adsorbent [30]. When the adsorbent dose was continuously increased to 0.5 g L⁻¹, the removal rate of Ni(II) tended to be stable. This may be due to the reduction in the concentration gradient between the adsorbate in the solution and adsorbate on the adsorbent surface [31]. It can be seen that the maximum adsorption was achieved when the adsorbent dose was 0.4 g L⁻¹, and the removal rate of Ni(II) on TWGAC was only 1.27% lower compared with NGAC.

3.3. Effect of pH on TWGAC and NGAC

The pH of the solution also has a major impact on the adsorption performance. The relationship between the removal rate of Ni(II) and pH is shown in Fig. 5b. These data suggest that the adsorption capacity of TWGAC and NGAC was greatly affected by pH but the overall trend was the same, which is in agreement with the experimental results of zeta potential. Furthermore, the adsorption capacity of TWGAC was not really different compared with NGAC at the same pH. When the pH was below 7, the removal rate of Ni(II) was low. However, it increased sharply as the initial pH increased from 7 to 7.5, and then grew gently in pH 7.5–9.0. According to some of the previously published work, the influence of pH on Ni(II) adsorption was mainly caused by the variation of H⁺ concentration [32,33]. At lower initial pH, excess H⁺ enhanced the competition with Ni(II). With the increase of pH, the functional groups on the surface are deprotonated, and the competition adsorption between Ni(II) and H⁺ became weak. The most basic interaction is, therefore, the strong electrostatic attraction between the metal cation Ni(II) and the deprotonated group [34]. Therefore, strong base environment is more favorable for the adsorption of Ni(II) by TWGAC and NGAC.

3.4. Effect of contact time on TWGAC and NGAC

The contact time plays an important role in the adsorption process. The relationship between the removal rate of Ni(II) and contact time is shown in Fig. 5c, demonstrating that the adsorption process of TWGAC and NGAC was very similar. Importantly, the removal rate of Ni(II) at the beginning of adsorption was relatively low. However, as the adsorption time increased, the removal rate also gradually increased. When the adsorption time continued to increase, the adsorption was close to the equilibrium and the removal rate appeared stable. This is because the adsorption of the adsorbate in the solution is a gradual process and it takes

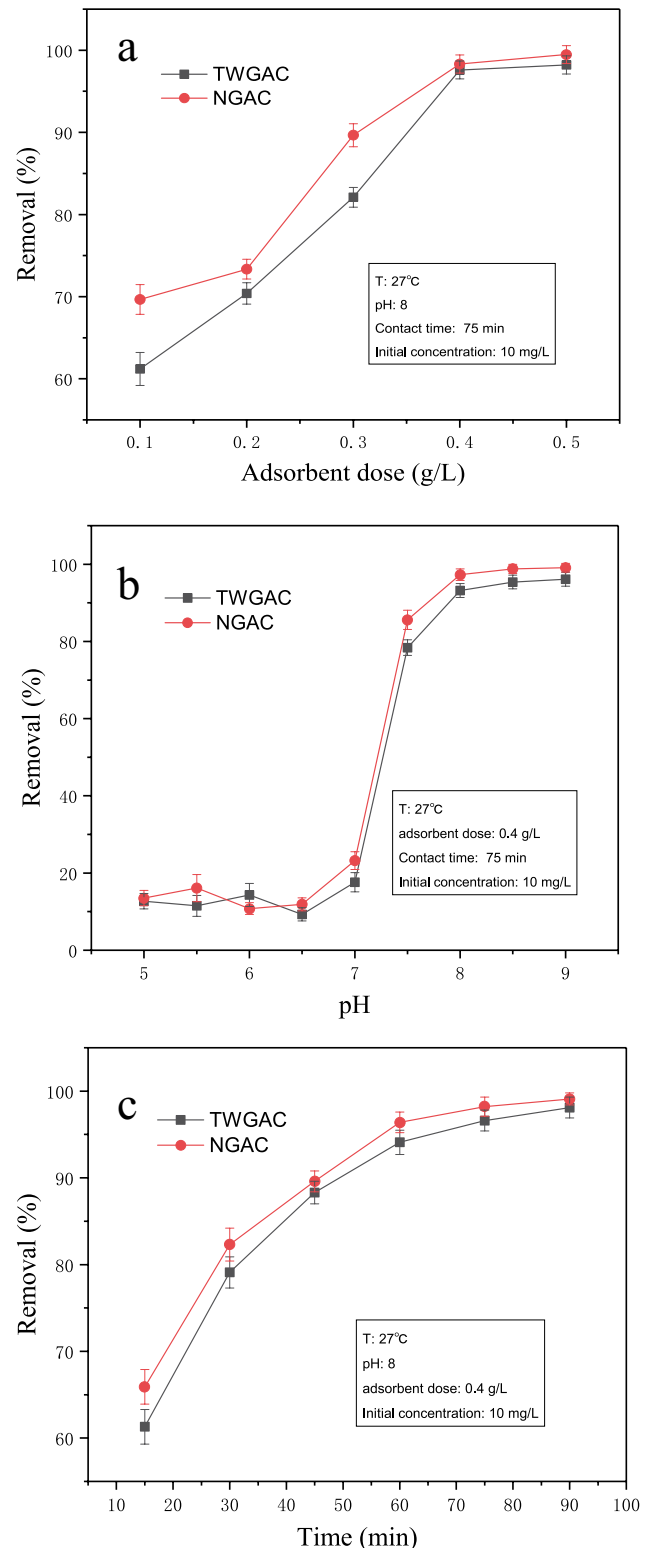


Fig. 5. (a) Effect of adsorbent dose on Ni(II) adsorption ($T = 27^{\circ}\text{C}$, $\text{pH} = 8$, contact time 75 min and adsorbate concentration 10 mg L⁻¹); (b) effect of pH on Ni(II) adsorption ($T = 27^{\circ}\text{C}$, adsorbate concentration 10 mg L⁻¹, contact time 75 min and adsorbent dose 0.4 g L⁻¹); (c) effect of contact time on Ni(II) adsorption ($T = 27^{\circ}\text{C}$, $\text{pH} = 8$, adsorbent dose 0.4 g L⁻¹, and adsorbate concentration 10 mg L⁻¹).

time for the adsorption to reach the equilibrium. In the beginning, the initial amount of available active sites can be freely adsorbed, resulting in a rapid increase in the Ni(II) removal rate. However, as the adsorption site becomes gradually occupied by Ni(II), the rate of removal decreases

and the adsorption tends to be balanced [35]. Indeed, we have demonstrated here that 75 min is a balance time that is logically and economically advantageous. At this time point, the removal rates of TWGAC and NGAC were 98.1% and 99.1%, respectively.

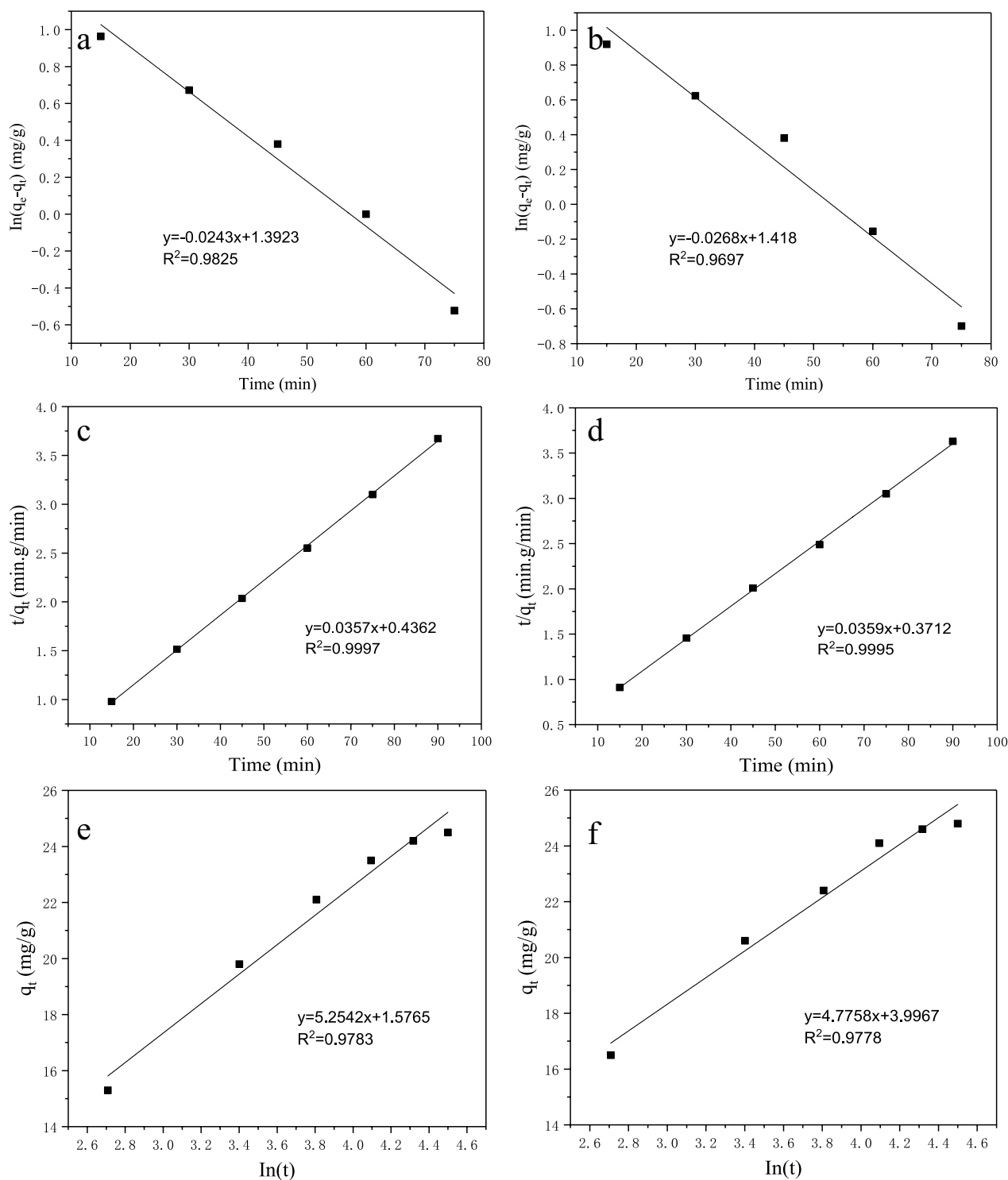


Fig. 6. Adsorption kinetics models: (a) pseudo-first-order model of Ni(II) on TWGAC; (b) pseudo-first-order model of Ni(II) on NGAC; (c) pseudo-second order-model of Ni(II) on TWGAC; (d) pseudo-second order-model of Ni(II) on NGAC; (e) Elovich model of Ni(II) on TWGAC; (f) Elovich model of Ni(II) on NGAC.

3.5. Adsorption kinetics

In order to evaluate the kinetic behavior of Ni(II) adsorption on TWGAC and NGAC, we utilized the fitting parameters of the three different models (Fig. 6 and Table 2). The fitting results show that TWGAC and NGAC have similar kinetic curves, which are largely due to the same material and similar particle size distribution. The pseudo-second-order kinetic model was more suitable for the adsorption process compared with the pseudo-first-order kinetic model. The correlation coefficients of the pseudo-second-order kinetic models of TWGAC and NGAC were 0.9997 and 0.9995, respectively. Furthermore, the fitted $q_{e,cal}$ was closer to the experimentally obtained $q_{e,exp}$. Therefore, the adsorption behavior of Ni(II) on TWGAC and NGAC follows a pseudo-secondary reaction mechanism. The pseudo-second-order model assumes that chemisorption can control the rate determination step. Therefore, the adsorption process is mainly controlled by chemisorption and may involve the valence state of electron sharing or exchange between the adsorbent and the adsorbate [36].

The Elovich kinetic model is primarily used to describe the chemisorption process on the surface of a heterogeneous adsorbent. In addition, the Elovich dynamic model reveals the irregularities of the data neglected by other kinetic models and is suitable for processes with large activation energies during the reaction [37,38]. The desorption constants β of TWGAC and NGAC were 0.1903 and 0.2094 g mg⁻¹, respectively (Table 2). The low desorption constant indicates that the desorption rate was very slow and the process was almost irreversible [39]. In addition, the β value of TWGAC was lower compared with NGAC, indicating that TWGAC might have a better interaction with Ni(II).

3.6. Adsorption isotherm

Studies of adsorption isotherms can aid in understanding of the number of sites of adsorption activity and the nature of the adsorbate–adsorbent interaction [39]. The Langmuir adsorption model assumes that the adsorbed molecules

Table 2
Kinetic constants of TWGAC and NGAC for Ni(II) adsorption

Kinetic models	Parameters	TWGAC	NGAC
Pseudo-first-order model	$q_{e,exp}$ (mg g ⁻¹)	24.5	24.8
	$q_{e,cal}$ (mg g ⁻¹)	4.02	4.13
	K_1 (min ⁻¹)	0.0243	0.0268
	R^2	0.9825	0.9697
Pseudo-second-order model	$q_{e,exp}$ (mg g ⁻¹)	24.5	24.8
	$q_{e,cal}$ (mg g ⁻¹)	28.01	27.85
	K_2 (min ⁻¹)	0.0029	0.0035
	R^2	0.9997	0.9995
Elovich model	α (mg g ⁻¹ min ⁻¹)	7.0925	6.4467
	β (g mg ⁻¹)	0.1903	0.2094
	R^2	0.9783	0.9778

occur on a uniform surface with a limited number of adsorption sites, as evidenced by the absence of interaction of the single-layer adsorption between the adsorbed molecules. In contrast, the Freundlich adsorption model assumes that the adsorption equilibrium conditions occur at heterogeneous sites with different adsorption energies, and the process of infinite adsorption is spontaneously formed [40,41]. The adsorption isotherms for adsorption of Ni(II) on TWGAC and NGAC at 27°C is shown in Fig. 7. The results of the fitting of two different isothermal models are shown in Fig. 8 and Table 3. The adsorption isotherm results of TWGAC and NGAC are more suitable for the Freundlich model by comparison of R^2 , indicating that multilayer (physical) adsorption occurred on the adsorbent surface [42]. From the Langmuir model, the maximum adsorption capacity of TWGAC and NGAC was 138.9 and 123.5 mg g⁻¹ at 27°C, respectively. Because TWGAC is ground into a fine powder and the contact with the adsorbate is increased, it may explain why its maximum adsorption capacity is slightly higher compared with NGAC. The Freundlich model is used to prove the heterogeneous system and assumes that the adsorption process is reversible [43]. The value of n can indicate the degree of non-linearity between the concentration of nickel in the solution and the nickel adsorbed. When $n < 2$, adsorption is unfavorable, and when $2 < n < 10$, adsorption is advantageous [44]. The obtained n values were 2.1 and 2.8 by fitting the experimental data of TWGAC and NGAC, respectively. This confirms that although the adsorption capacity of TWGAC was decreased, it was still beneficial.

3.7. Adsorption thermodynamics

Thermodynamic studies increase the insight into the type and mechanism of the adsorption process. The adsorption thermodynamic parameters, including the Gibbs free energy, enthalpy, and entropy were calculated (Table 4). Both ΔG values of TWGAC and NGAC were negative, indicating that the Ni(II) adsorption was spontaneous. Specifically,

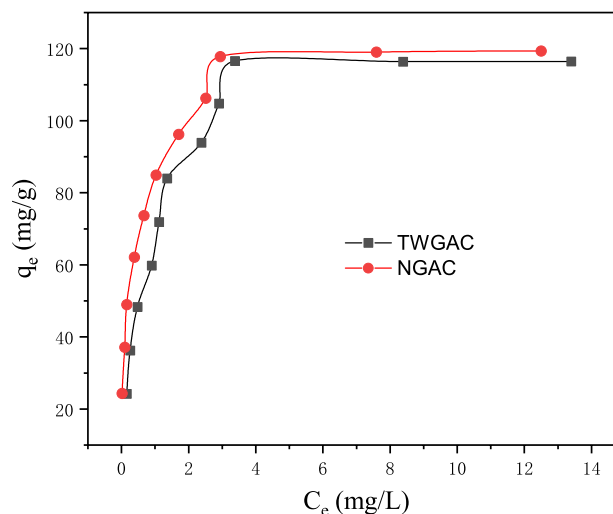


Fig. 7. Adsorption isotherms of Ni(II) on TWGAC and NGAC.

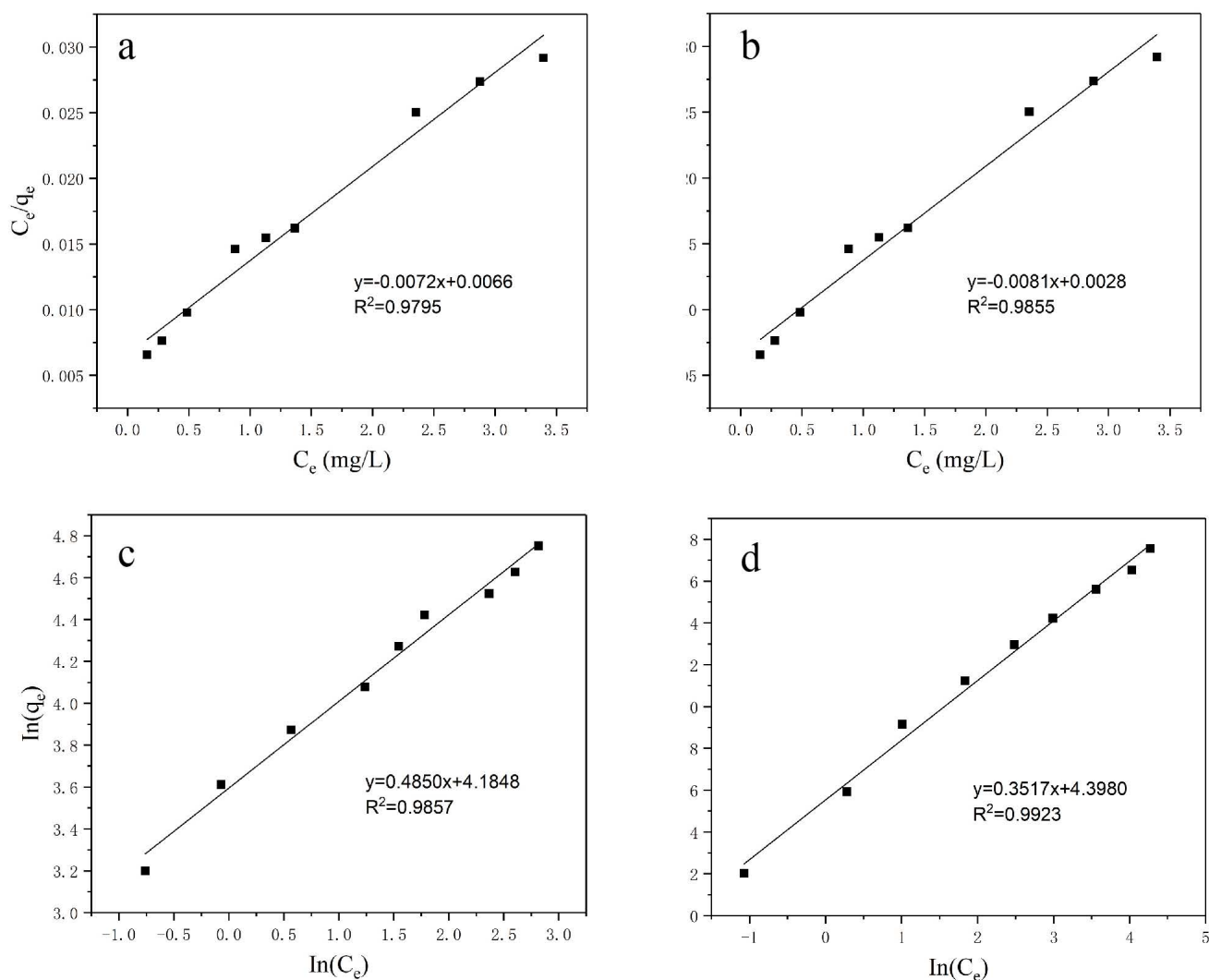


Fig. 8. Adsorption isotherm models: (a) Langmuir model of Ni(II) on TWGAC; (b) Langmuir model of Ni(II) on NGAC; (c) Freundlich model of Ni(II) on TWGAC; (d) Freundlich model of Ni(II) on NGAC.

Table 3
Adsorption of Ni(II) parameters and coefficients on TWGAC and NGAC by two different isotherm models

Isotherm models	Constant	TWGAC	NGAC
Langmuir model	q_m (mg g ⁻¹)	138.9	123.5
	K_L (L mg ⁻¹)	1.1	2.9
	R^2	0.9795	0.9855
Freundlich model	n	2.1	2.8
	K_F	65.7	81.3
	R^2	0.9857	0.9923

Table 4
Adsorption thermodynamic parameters for Ni(II) adsorption on TWGAC and NGAC

Adsorbent	T (°C)	ΔG (kJ mol ⁻¹)	ΔH (kJ mol ⁻¹)	ΔS (kJ mol ⁻¹ K ⁻¹)
TWGAC	27	-10.44	0.002	0.0348
	37	-10.78		
	47	-11.13		
NGAC	27	-10.969	0.011	0.0366
	37	-11.335		
	47	-11.701		

the external energy of the system was not required for the adsorption process [44]. Next, the ΔG value decreased with increasing temperature and a positive value of ΔH , indicating that the adsorption of Ni(II) was an endothermic process, which means that the adsorption of Ni(II) on the TWGAC

and NGAC increased as the temperature increased [45]. Moreover, a positive value of ΔS indicates that Ni(II) has a good affinity for these two adsorbents and is stable at the adsorption site [46].

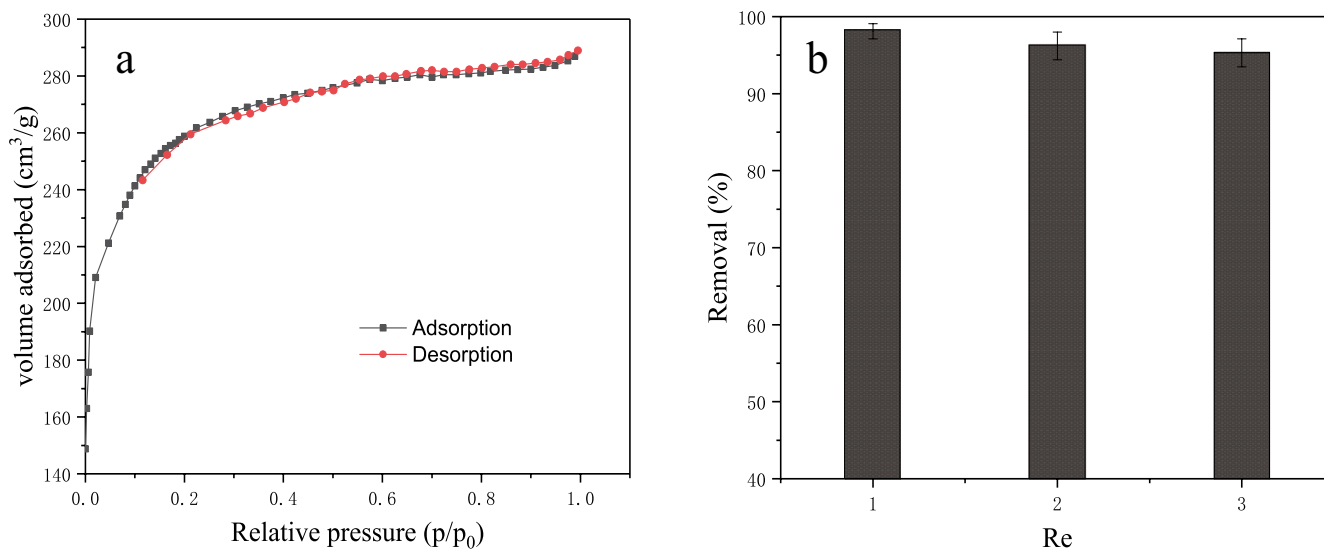


Fig. 9. (a) Ni(II) removal rate of three reuse cycles; (b) nitrogen adsorption–desorption isotherm of TWGAC after the last reuse cycle.

3.8. Reuse of TWGAC

In order to understand the application potential of TWGAC, the reusability of the exhausted TWGAC was examined. Specifically, we washed saturated TWGAC powder under ultrasonic waves at 40 kHz for 10 min, followed by drying at 105°C. The initial adsorption mass concentration, amount of adsorbent, temperature, and pH were controlled at 10 mg L⁻¹, 0.4 g L⁻¹, 27°C, and 8, respectively, and the experiment was carried out for a total of three adsorption and reuse cycles. The experimental results and the nitrogen adsorption–desorption curve of the activated carbon after the last use are shown in Fig. 9. TWGAC is still described as a type I isotherm after three cycles of use. However, its specific surface area has decreased to 865.71 m² g⁻¹. The results also showed that the removal rate decreased from 98.1% to 95.3% after three cycles, but the TWGAC still had a good adsorption capacity. The stable removal rate further proves that the TWAAC used in this study has the potential to remove Ni(II).

4. Conclusion

In this paper, WGAC was treated by ultrasonic cleaning, drying, and grinding, and it was successfully used to adsorb Ni(II) from water. According to the comparison with the NGAC under the N₂ adsorption/desorption isotherms, SEM, EDS, FTIR, particle size distribution and zeta potential, the structure of WGAC was severely damaged and was not suitable for regeneration. However, it still had a high specific surface area (893.37 m² g⁻¹) and a good adsorption capacity. In addition, the treatment used in this study was able to remove impurities from the WGAC and restore functional groups. Compared with NGAC, TWGAC had less adsorption capacity under the same conditions, and both were affected by the same factors and used under optimal operation. The adsorption performance of TWGAC and NGAC for Ni(II) was greatly affected by pH, and the adsorption performance was better under strong alkali conditions. The experimental data of TWGAC and NGAC

were overall consistent with the adsorption kinetics, isotherms and thermodynamics, indicating that the adsorption mechanism of WGAC after treatment did not change. The adsorption process can be described by a pseudo-second-order kinetic model. The adsorption isotherm results of TWGAC and NGAC were well fitted using the Freundlich model, and the maximum adsorption capacity q_m of Ni(II) were 138.9 and 123.5 mg g⁻¹ for TWGAC and NGAC, respectively. Thermodynamic analysis suggested that the values of ΔG and ΔH on the adsorption of Ni(II) by TWGAC and NGAC were essentially physical and a spontaneous and endothermic process. A positive value of ΔS suggested that TWGAC and NGAC had a good affinity for Ni(II). The TWGAC can be reused as an adsorbent at least three times before the final disposal. In summary, the methods presented herein can be used to economically and efficiently reuse WGAC units that are not conducive to regeneration. TWGAC is superior to many adsorbents in heavy metal adsorption and has great application potential in future practical engineering.

Acknowledgments

The authors would like to express their sincere gratitude to the National Natural Science Foundation of China (51608272), the Postgraduate Research & Practice Innovation Program of Jiangsu Province (KYCX18_0973), the Science and Technology Project of Jiangsu Provincial Department of Housing and Urban-Rural Development (2017ZD055) and a project funded by the Priority Academic Program Development of the Jiangsu Higher Education Institutions (PAPD) for financial support.

References

- [1] W.W. Gong, Y.J. Yu, G. Liang, X.H. Liu, B.S. Cui, J.H. Bai, P. Han, Factor effects and mechanisms of the adsorption of Hg(II), Cd(II) and Ni(II) on charged liposomes, *Colloids Surf., A*, 538 (2018) 460–466.
- [2] X.L. Wang, L.Z. Song, C.L. Tian, J.H. He, S.J. Wang, J.B. Wang, C.Y. Li, DFT investigation of the effects of coexisting cations

- and complexing reagents on Ni(II) adsorption by a polyvinylidene fluoride-type chelating membrane bearing poly (amino phosphonic acid) groups, *Metals*, 7 (2017) 61.
- [3] L. Wang, R.T. Liu, Y. Teng, Study on the toxic interactions of Ni²⁺ with DNA using neutral red dye as a fluorescence probe, *J. Lumin.*, 131 (2011) 705–709.
- [4] S. Vilvanathan, S. Shanthakumar, Column adsorption studies on nickel and cobalt removal from aqueous solution using native and biochar form of *Tectona grandis*, *Environ. Prog. Sustainable Energy*, 34 (2017) 1030–1038.
- [5] World Health Organization, *Guidelines for Drinking-Water Quality*, World Health Organization, Geneva, 1996.
- [6] J. Liu, Z.F. Qiu, J. Yang, L.M. Cao, W. Zhang, Recovery of Mo and Ni from spent acrylonitrile catalysts using an oxidation leaching–chemical precipitation technique, *Hydrometallurgy*, 164 (2016) 64–70.
- [7] N.K. Amin, O. Abdelwahab, E.-S.Z. El-Ashtouky, Removal of Cu(II) and Ni(II) by ion exchange resin in packed rotating cylinder, *Desal. Wat. Treat.*, 55 (2015) 199–209.
- [8] Y.Y. Ge, Y. Yuan, K.T. Wang, Y. He, X.M. Cui, Preparation of geopolymer-based inorganic membrane for removing Ni²⁺ from wastewater, *J. Hazard. Mater.*, 299 (2015) 711–718.
- [9] Y. Zhou, Z.-h. Yang, J. Huang, R. Xu, P.-p. Song, Y.-j. Zhang, J. Li, M. Aloun, Ni(II) removal from aqueous solution by biosorption and flocculation using microbial flocculant GA1, *Res. Chem. Intermed.*, 43 (2017) 3939–3959.
- [10] N.P.G.N. Chandrasekara, R.M. Pashley, Study of a new process for the efficient regeneration of ion exchange resins, *Desalination*, 357 (2015) 131–139.
- [11] H.B. Wang, W. Wang, Y.F. Zhao, Z.W. Xu, L. Chen, L.H. Zhao, X. Tian, W.Y. Sun, Superior adsorption of 3D nanoporous architectures for Ni(II) ions adsorption using polyvinyl alcohol as cross-linking agent and adsorption conveyor, *RSC Adv.*, 8 (2018) 7899–7903.
- [12] B. Liberman, Three methods of forward osmosis cleaning for RO membranes, *Desalination*, 431 (2018) 22–26.
- [13] M. Ferhat, S. Kadouche, H. Lounici, Immobilization of heavy metals by modified bentonite coupled coagulation/flocculation process in the presence of a biological flocculant, *Desal. Wat. Treat.*, 57 (2016) 6072–6080.
- [14] P. Loganathan, W.G. Shim, D.P. Sountharajah, M. Kalaruban, T. Nur, S. Vigneswaran, Modelling equilibrium adsorption of single, binary, and ternary combinations of Cu, Pb, and Zn onto granular activated carbon, *Environ. Sci. Pollut. Res.*, 25 (2018) 16664–16675.
- [15] R. Cherbański, Regeneration of granular activated carbon loaded with toluene – Comparison of microwave and conductive heating at the same active powers, *Chem. Eng. Process.*, 123 (2018) 148–157.
- [16] Y. Li, H.L. Jin, W.B. Liu, H. Su, Y. Lu, J.F. Li, Study on regeneration of waste powder activated carbon through pyrolysis and its adsorption capacity of phosphorus, *Sci. Rep.*, 8 (2018) 778.
- [17] M. El Gamal, H.A. Mousa, M.H. El-Naas, R. Zacharia, S. Judd, Bio-regeneration of activated carbon: a comprehensive review, *Sep. Purif. Technol.*, 197 (2018) 345–359.
- [18] K.Y. Foo, Effect of microwave regeneration on the textural network, surface chemistry and adsorptive property of the agricultural waste based activated carbons, *Process Saf. Environ. Prot.*, 116 (2018) 461–467.
- [19] I. Benhamed, L. Barthe, R. Kessas, C. Julcour, H. Delmas, Effect of transition metal impregnation on oxidative regeneration of activated carbon by catalytic wet air oxidation, *Appl. Catal., B*, 187 (2016) 228–237.
- [20] S. Roman, B. Ledesma, J.F. González, A. Al-Kassir, G. Engo, A. Álvarez-Murillo, Two stage thermal regeneration of exhausted activated carbons. Steam gasification of effluents, *J. Anal. Appl. Pyrolysis*, 103 (2013) 201–206.
- [21] Z.H. Sun, C. Liu, Z. Cao, W. Chen, Study on regeneration effect and mechanism of high-frequency ultrasound on biological activated carbon, *Ultrason. Sonochem.*, 44 (2018) 86–96.
- [22] J. Rouquerol, F. Rouquerol, K.S.W. Sing, P. Llewellyn, G. Maurin, *Adsorption by Powders and Porous Solids: Principles, Methodology and Applications*, Academic Press, New York, 2014.
- [23] S. Lowell, J. Shields, M.A. Thomas, M. Thommes, *Characterization of Porous Solids and Powders: Surface Area, Porosity and Density*, Springer, Dordrecht, 2004.
- [24] M. Thommes, K. Kaneko, A.V. Neimark, J.P. Olivier, F. Rodriguez-Reinoso, J. Rouquerol, K.S.W. Sing, *Physisorption of gases, with special reference to the evaluation of surface area and pore size distribution (IUPAC Technical Report)*, *Pure Appl. Chem.*, 87 (2015) 1051–1069.
- [25] J. Rouquerol, P. Llewellyn, F. Rouquerol, Is the BET equation applicable to microporous adsorbents?, P.L. Llewellyn, F. Rodriguez-Reinoso, J. Rouquerol, N. Seaton, Eds., *Studies in Surface Science and Catalysis*, Elsevier, Amsterdam, 2007, pp. 49–56.
- [26] W.L. Wang, Y. Liu, X.H. Liu, B.J. Deng, S.Y. Lu, Y.R. Zhang, B. Bi, Z.M. Ren, Equilibrium adsorption study of the adsorptive removal of Cd²⁺ and Cr⁶⁺ using activated carbon, *Environ. Sci. Pollut. Res.*, 25 (2018) 25538–25550.
- [27] Z. Wang, L. Chen, Adsorption characteristics of dibutyl phthalate from aqueous solution using ginkgo leaves-activated carbon by chemical activation with zinc chloride, *Desal. Wat. Treat.*, 54 (2015) 1969–1980.
- [28] J.J. Kong, Q.Y. Yue, L.H. Huang, Y. Gao, Y.Y. Sun, B.Y. Gao, Q. Li, Y. Wang, Preparation, characterization and evaluation of adsorptive properties of leather waste based activated carbon via physical and chemical activation, *Chem. Eng. J.*, 221 (2013) 62–71.
- [29] X. Yang, H.H. Yi, X.L. Tang, S.Z. Zhao, Z.Y. Yang, Y.Q. Ma, T.C. Feng, X.X. Cui, Behaviors and kinetics of toluene adsorption-desorption on activated carbons with varying pore structure, *J. Environ. Sci.*, 67 (2018) 104–114.
- [30] M. Dehghani, M. Nozari, I. Golkari, N. Rostami, M.A. Shiri, Adsorption and kinetic studies of hexavalent chromium by dehydrated *Scrophularia striata* stems from aqueous solutions, *Desal. Wat. Treat.*, 125 (2018) 81–92.
- [31] A.R. Kaveeshwar, S.K. Ponnusamy, E.D. Revellame, D.D. Gang, M.E. Zappi, R. Subramaniam, Pecan shell based activated carbon for removal of iron(II) from fracking wastewater: adsorption kinetics, isotherm and thermodynamic studies, *Process Saf. Environ. Prot.*, 114 (2018) 107–122.
- [32] E. Bibaj, K. Lysigaki, J.W. Nolan, M. Seyedsalehi, E.A. Deliyanni, A.C. Mitropoulos, G.Z. Kyzas, Activated carbons from banana peels for the removal of nickel ions, *Int. J. Environ. Sci. Technol.*, 16 (2019) 667–680.
- [33] Y.R. Li, J. Zhang, H. Liu, In-situ modification of activated carbon with ethylenediaminetetraacetic acid disodium salt during phosphoric acid activation for enhancement of nickel removal, *Powder Technol.*, 325 (2018) 113–120.
- [34] J. Zolgharnein, M. Bagtash, S. Feshki, P. Zolgharnein, D. Hammond, Crossed mixture process design optimization and adsorption characterization of multi-metal (Cu(II), Zn(II) and Ni(II)) removal by modified *Buxus sempervirens* tree leaves, *J. Taiwan Inst. Chem. Eng.*, 7 (2017) 104–117.
- [35] K. Senthilkumar, V.C. Devi, S. Mothil, M.N. Kumar, Adsorption studies on treatment of textile wastewater using low-cost adsorbent, *Desal. Wat. Treat.*, 123 (2018) 90–100.
- [36] J.B. Yang, S.C. Han, Kinetics and equilibrium study for the adsorption of lysine on activated carbon derived from coconut shell, *Desal. Wat. Treat.*, 120 (2018) 261–271.
- [37] P.S. Kumar, S.J. Varjani, S. Suganya, Treatment of dye wastewater using an ultrasonic aided nanoparticle stacked activated carbon: Kinetic and isotherm modelling, *Bioresour. Technol.*, 250 (2018) 716–722.
- [38] G.H. Liu, Z.H. Zhang, C. Yan, Y. Wang, X.R. Ma, P. Gao, Y.J. Feng, Adsorption of estrone with few-layered boron nitride nanosheets: kinetics, thermodynamics and mechanism, *Chemosphere*, 207 (2018) 534–542.
- [39] Z. Wang, M.G. Zhong, L. Chen, Coal-based granular activated carbon loaded with MnO₂ as an efficient adsorbent for removing formaldehyde from aqueous solution, *Desal. Wat. Treat.*, 57 (2016) 13225–13235.
- [40] Z. Wang, Efficient adsorption of dibutyl phthalate from aqueous solution by activated carbon developed from phoenix leaves, *Int. J. Environ. Sci. Technol.*, 12 (2015) 1923–1932.

- [41] J. Yin, C.B. Deng, Z. Yu, X.F. Wang, G.P. Xu, Effective removal of lead ions from aqueous solution using nano illite/smectite clay: isotherm, kinetic, and thermodynamic modeling of adsorption, *Water*, 10 (2018) 210.
- [42] D. Tiwari, H. Bhunia, P.K. Bajpai, Development of chemically activated N-enriched carbon adsorbents from urea-formaldehyde resin for CO₂ adsorption: Kinetics, isotherm, and thermodynamics, *J. Environ. Manage.*, 218 (2018) 579–592.
- [43] W. Lee, S. Yoon, J.K. Choe, M. Lee, Y. Choi, Anionic surfactant modification of activated carbon for enhancing adsorption of ammonium ion from aqueous solution, *Sci. Total Environ.*, 639 (2018) 1432–1439.
- [44] B. Sadeghalvad, A.R. Azadmehr, H. Motevalian, Statistical design and kinetic and thermodynamic studies of Ni(II) adsorption on bentonite, *J. Central South Univ.*, 24 (2017) 1529–1536.
- [45] Z.Q. Jing, Y.Y. Peng, R. He, Y. Xu, T. Yu, J. Hu, Poplar leaves reclamation for porous granules and their application in nitrobenzene removal from aqueous solution, *Desal. Wat. Treat.*, 57 (2016) 449–459.
- [46] A.K. Kushwaha, N. Gupta, M.C. Chattopadhyaya, Dynamics of adsorption of Ni(II), Co(II) and Cu(II) from aqueous solution onto newly synthesized poly[N-(4-[4-(aminophenyl)methylphenylmethacrylamide])], *Arabian J. Chem.*, 10 (2017) S1645–S1653.